Kunz, M. & Brown, I. D. (1995). *J. Solid State Chem.* **115**, 395–406.

Maclean, D. A., Ng, H. N. & Greedan, J. E. (1979). *J. Solid State Chem.* **30**, 35–44.

Richard, M., Brohan, L. & Tournoux, M. (1994). *J. Solid State Chem.* **112**, 345–354.

Ruddlesden, S. N. & Popper, P. (1958). *Acta Cryst.* **11**, 54–55.

Sheldrick, G. M. (1993a). *SHELXTL93.* Version 5.03. Siemens Analytical X-ray Instruments Inc., Madison, Wisconsin, USA.

Sheldrick, G. M. (1993b). *SHELXL93. Program for the Refinement of Crystal Structures.* University of Göttingen, Germany.

Sheldrick, G. M. (1996). *SADABS. Siemens Area Detector Absorption Correction Software.* University of Göttingen, Germany.

Siemens (1996). *SMART* and *SAINT.* Release 4.05. *Area Detector Control and Integration Software.* Siemens Analytical X-ray Instruments Inc., Madison, Wisconsin, USA.

Acta Cryst. (1998). C54, 1055–1057

$Na_3Mn_4Te_2O_{12}$

CHRISTOPHER R. FEGER AND JOSEPH W. KOLIS

Department of Chemistry, Clemson University, Clemson, SC 29634, USA. E-mail: kjoseph@clemson.edu

Abstract

The title compound, sodium manganese tellurate, was obtained by hydrothermal synthesis and adopts a super-structure related to the $CaFe_2O_4$ structure type, with the Mn and Te atoms ordered along the b axis (short axis in the $CaFe_2O_4$ structure). Electron-counting schemes show that this compound is a mixed-valence Mn^{II}/Mn^{III} compound, and bond valence sums are used to suggest that there is no site preference for the higher charged Mn atom.

Comment

There are a variety of AB_2X_4 compounds that adopt the $CaFe_2O_4$ structure type (Decker & Kasper, 1957). Some typical metal oxides include $CaCr_2O_4$ (Hörkner & Müller-Buschbaum, 1976), CaV_2O_4 (Bertaut *et al.*, 1955) and $NaTi_2O_4$ (Akimoto & Takei, 1989). Many rare earth sulfides, such as $BaSm_2S_4$ (Carpenter & Hwu, 1992), also crystallize with this structure type. There are also several cases where the B site is populated by several types of atoms, most notably in $NaScMO_4$ (M = Ti, Zr, Hf, Sn) (Reid *et al.*, 1968). In these compounds, there is a random distribution of Sc atoms and the tetravalent metal in the B sites. Upon determination of the structure of $Na_3Mn_4Te_2O_{12}$, we have found, to the best of our knowledge, the first compound that adopts a superstructure of the $CaFe_2O_4$ structure type, with the

unit cell tripled as a result of the ordering of the Mn and Te atoms along the b axis. Columns are made up of repeating groups of edge-sharing octahedra along the b axis. These columns have a repeat sequence of MnO_6–TeO_6–MnO_6, and are linked to one another through shared vertices, forming channels that contain the Na atoms. A typical repeating group is shown in Fig. 1, and a polyhedral view of the unit cell of the title compound is shown in Fig. 2.
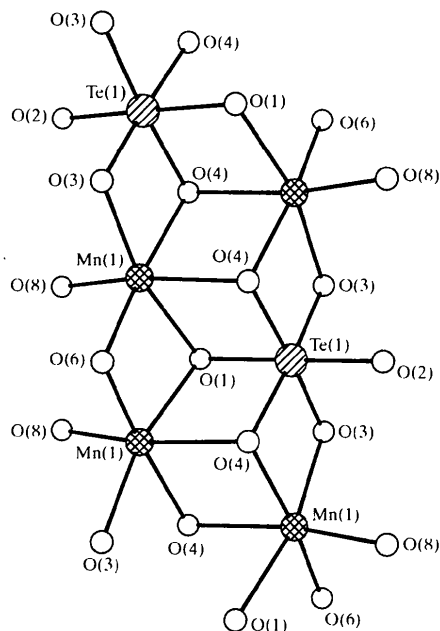

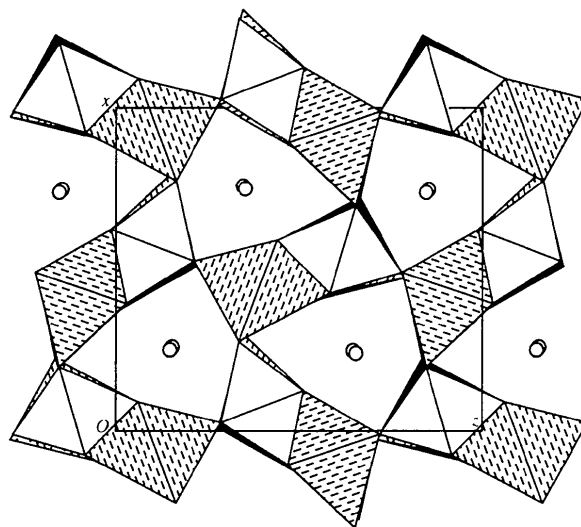Fig. 1. The repeat sequence of edge-sharing octahedra.

Fig. 2. Polyhedral representation of $Na_3Mn_4Te_2O_{12}$ viewed down the b axis. MnO_6 octahedra are dashed and TeO_6 octahedra are blank. The isolated spheres are Na atoms. The edge-sharing pairs of octahedra at the origin and center of the unit cell contain the Mn(2) and Te(2) atoms. The pairs that contain the Mn(1) and Te(1) atoms are located at $(0, y, \frac{1}{2})$ and $(\frac{1}{2}, y, 0)$.

Although there is a size difference between the Mn and Te sites within their respective octahedra, this alone is not sufficient to account for the ordering of the transition metal atoms. The sizable difference in oxidation states, $Mn^{2.25+}$ and Te^{6+}, prevents tellurium from occupying adjacent octahedra, which would otherwise cause overbonding of the shared O atoms. The Te—O distances range from 1.916 (9) to 1.958 (12) Å, which are comparable to the sum of Te and O crystal radii (1.96 Å) (Shannon, 1976). Similarly, there is reasonable agreement between the calculated value (2.07 Å) and the experimental values [2.057 (9)–2.219 (10) Å] for Mn—O bonds.

By assuming the common oxidation states of +1 and −2 for Na and O, respectively, and assigning the oxidation states of all octahedrally coordinated Te atoms as +6, there are nine remaining positive charges which must be distributed over four Mn atoms in two crystallographically distinct environments. Bond valence sums (Brown & Altermatt, 1985) were used to ascertain whether the additional positive charge is localized in either site. The bond valence sums were calculated using the value for an Mn^{II}—O^{II} bond; sums of 2.39 (3) and 2.21 (2) were obtained for the Mn(1) and Mn(2) atoms, respectively, which suggests that the Mn^{III} atom is randomly distributed over the two Mn sites.

Experimental

Crystals of $Na_3Mn_4Te_2O_{12}$ were prepared from MnO_2 (71 mg, Strem, 99%) and $Te(OH)_6$ (375 mg, Strem, 99.9%). The reagents and 5.3 ml of 1 M NaOH solution were placed in a stainless-steel autoclave (approximate volume 10.6 ml) and heated at 648 K for 5 d. After cooling the autoclave, the products were filtered and washed once with distilled water and twice with acetone. The title compound was obtained as brown needles in 30% yield (estimated by volume). In attempts to optimize yields with stoichiometric amounts of the reagents, no detectable level of the desired product was obtained. Qualitative EDAX verified the presence of sodium, manganese, tellurium and oxygen, and the absence of impurities heavier than oxygen.

Crystal data

$Na_3Mn_4Te_2O_{12}$	Mo $K\alpha$ radiation
$M_r = 735.91$	$\lambda = 0.71073$ Å
Orthorhombic	Cell parameters from 25
$Pnma$	reflections
$a = 9.384\,(2)$ Å	$\theta = 13.25–18.96°$
$b = 9.182\,(2)$ Å	$\mu = 11.455$ mm^{-1}
$c = 10.997\,(3)$ Å	$T = 295$ K
$V = 947.5\,(7)$ Å^3	Rod
$Z = 4$	$0.10 \times 0.02 \times 0.02$ mm
$D_x = 5.158$ Mg m^{-3}	Brown
D_m not measured	

Data collection

Rigaku AFC-7R diffractometer	884 reflections with $F > 2\sigma(F)$
ω–2θ scans	$R_{int} = 0.034$
Absorption correction:	$\theta_{max} = 27.50°$
empirical via ψ scans	$h = 0 \rightarrow 12$
(North et al., 1968)	$k = -11 \rightarrow 11$
$T_{min} = 0.32$, $T_{max} = 0.80$	$l = -14 \rightarrow 14$
2422 measured reflections	3 standard reflections
1157 independent reflections	every 100 reflections
	intensity decay: 1.11%

Refinement

Refinement on F	$\Delta\rho_{max} = 4.35$ e Å^{-3}
$R = 0.048$	$\Delta\rho_{min} = -2.96$ e Å^{-3}
$wR = 0.049$	Extinction correction:
$S = 2.64$	Larson (1970)
884 reflections	Extinction coefficient:
107 parameters	0.00005 (1)
$w = 1/[\sigma^2(F) + 0.002F^2]$	Scattering factors from
$(\Delta/\sigma)_{max} = 0.001$	Cromer & Waber (1974)

Table 1. *Selected bond distances (Å)*

Te(1)—O(1)	1.958 (12)	Mn(2)—O(5^{iv})	2.201 (11)
Te(1)—O(2)	1.940 (14)	Mn(2)—O(7)	2.190 (10)
Te(1)—O(3)	1.916 (9)	Mn(2)—O(7^{iv})	2.154 (7)
Te(1)—O(3^i)	1.916 (9)	Mn(2)—O(8)	2.150 (10)
Te(1)—O(4)	1.952 (10)	Na(1)—O(4)	2.379 (11)
Te(1)—O(4^i)	1.952 (10)	Na(1)—O(4^i)	2.379 (11)
Te(2)—O(5)	1.954 (12)	Na(1)—O(6)	2.721 (14)
Te(2)—O(6)	1.932 (12)	Na(1)—O(6^{ii})	2.459 (15)
Te(2)—O(7)	1.936 (9)	Na(1)—O(7)	2.374 (11)
Te(2)—O(7^i)	1.936 (9)	Na(1)—O(7^i)	2.374 (11)
Te(2)—O(8)	1.933 (10)	Na(1)—O(8^v)	2.549 (11)
Te(2)—O(8^i)	1.933 (10)	Na(1)—O(8^{vi})	2.549 (11)
Mn(1)—O(1^{ii})	2.145 (9)	Na(2)—O(1^{ii})	2.442 (11)
Mn(1)—O(3)	2.102 (10)	Na(2)—O(2^v)	2.608 (12)
Mn(1)—O(4)	2.164 (10)	Na(2)—O(3^{ii})	2.618 (12)
Mn(1)—O(4^{ii})	2.219 (10)	Na(2)—O(3^v)	2.688 (10)
Mn(1)—O(6^{iii})	2.057 (9)	Na(2)—O(4)	2.473 (11)
Mn(1)—O(8^{iv})	2.17 (10)	Na(2)—O(5^{iv})	2.373 (12)
Mn(2)—O(2^{iv})	2.149 (10)	Na(2)—O(7)	2.414 (11)
Mn(2)—O(3^v)	2.126 (9)		

Symmetry codes: (i) $x, \frac{1}{2} - y, z$; (ii) $-x, -y, 1 - z$; (iii) $\frac{1}{2} - x, -y, z - \frac{1}{2}$; (iv) $1 - x, -y, 1 - z$; (v) $\frac{1}{2} - x, -y, \frac{1}{2} + z$; (vi) $x - \frac{1}{2}, y, \frac{3}{2} - z$; (vii) $x - \frac{1}{2}, \frac{1}{2} - y, \frac{3}{2} - z$.

The Mn and Te atoms were located by direct methods, and the Na and O atoms were located by progressive difference Fourier maps. After all peaks were assigned, all atoms were refined anisotropically. Due to the large, elongated displacement ellipsoid of the Mn(2) atom, a refinement was attempted with two half-occupied sites 0.5 Å apart. This model was rejected, as the two sites coalesced to the original site. A large number (~25%) of the observed reflections were excluded when a cutoff of $F > 2\sigma(F)$ was employed. Exclusion of these reflections resulted in a somewhat low observation-to-parameter ratio with large S and $\Delta\rho$ values. All but four of these reflections were observed when an $F > \sigma(F)$ cutoff was employed. When this new cutoff was used, there was a decrease in S from 2.64 to 2.31; however, the R and wR factors and the $\Delta\rho$ values increased. It is believed that this high percentage of weak but real reflections is responsible for the somewhat poor refinement parameters. Due to larger values of R, wR and $\Delta\rho$, combined with only modest improvements

of S and relatively minor changes in the positional parameters, displacement ellipsoids, and their standard uncertainties, the original $F > 2\sigma(F)$ cutoff was used in the final structure refinement. The maximum and minimum residual electron-density peaks were located 0.74 Å from Te(2) and 0.89 Å from Te(1), respectively.

Data collection: *MSC/AFC Diffractometer Control Software* (Molecular Structure Corporation, 1988). Cell refinement: *MSC/AFC Diffractometer Control Software*. Data reduction: *TEXSAN* (Molecular Structure Corporation, 1993). Program(s) used to solve structure: *SHELXS86* (Sheldrick, 1985). Program(s) used to refine structure: *SHELXTL-Plus* (Sheldrick, 1990). Molecular graphics: *SHELXTL-Plus*.

References

Akimoto, J. & Takei, H. (1989). *J. Solid State Chem.* **79**, 212–217.
Bertaut, E. F., Blum, P. & Magnano, G. (1955). *C. R. Acad. Sci. Paris*, **241**, 757–759.
Brown, I. D. & Altermatt, D. (1985). *Acta Cryst.* **B41**, 244–247.
Carpenter, J. D. & Hwu, S.-J. (1992). *Acta Cryst.* **C48**, 1164–1167.
Cromer, D. T. & Waber, J. T. (1974). *International Tables for X-ray Crystallography*, Vol. IV, Table 2.2A. Birmingham: Kynoch Press. (Present distributor Kluwer Academic Publishers, Dordrecht.)
Decker, B. F. & Kasper, J. S. (1957). *Acta Cryst.* **10**, 332–337.
Hörkner, W. & Müller-Buschbaum, H. (1976). *Z. Naturforsch. Teil B*, **31**, 1710–1711.
Larson, A. C. (1970). *Crystallographic Computing*, edited by F. R. Ahmed, S. R. Hall & C. P. Huber, pp. 291–294. Copenhagen: Munksgaard.
Molecular Structure Corporation (1988). *MSC/AFC Diffractometer Control Software*. MSC, 3200 Research Forest Drive, The Woodlands, TX 77381, USA.
Molecular Structure Corporation (1993). *TEXSAN. Single Crystal Structure Analysis Software*. Version 1.6b. MSC, 3200 Research Forest Drive, The Woodlands, TX 77381, USA.
North, A. C. T., Phillips, D. C. & Mathews, F. S. (1968). *Acta Cryst.* **A24**, 351–359.
Reid, A. F., Wadsley, A. D. & Sienko, M. J. (1968). *Inorg. Chem.* **7**, 112–118.
Shannon, R. D. (1976). *Acta Cryst.* **A32**, 751–767.
Sheldrick, G. M. (1985). *SHELXS86. Crystallographic Computing 3*, edited by G. M. Sheldrick, C. Krüger & R. Goddard, pp. 175–189. Oxford University Press.
Sheldrick, G. M. (1990). *SHELXTL-Plus*. Version 4.0. Siemens Analytical X-ray Instruments Inc., Madison, Wisconsin, USA.

A Neodymium-Substituted Britholite Compound

LAURENT BOYER,[a] JEAN-MICHEL SAVARIAULT,[b] JOËLLE CARPENA[a] AND JEAN-LOUIS LACOUT[c]

[a]*Laboratoire d'Etudes des Matrices de Confinement–CEA, Service d'Etudes Procédés, CEN Cadarache, 13108 Saint Paul Lez Durance, France,* [b]*Centre d'Elaboration de Matériaux et d'Etudes Structurales–CNRS, 29 rue Jeanne Marvig, BP 4347, 31055 Toulouse CEDEX, France, and* [c]*Laboratoire d'Etudes Physico-Chimiques des Phosphates, 38 rue des 36 Ponts, 31400 Toulouse, France. E-mail: savariau@cemes.cemes.fr*

Abstract

A single crystal of calcium neodymium fluoride oxide phosphate silicate, $Ca_9Nd(PO_4)_5(SiO_4)F_{1.5}O_{0.25}$, was obtained by a synthesis involving the heating of a $CaF_2/P_2O_5/CaCO_3/Nd_2O_3/SiO_2$ mixture at 1973 K over a period of 2 h followed by cooling at 50 K min⁻¹. The structure is of the britholite type, a mixed silica–phosphate apatite. The neodymium is distributed over both calcium sites, 17% in calcium site I and 83% in calcium site II. The channel which contains the anions is partially filled with 77% F^- and 13% O^{2-}, the remaining 10% being vacancies.

Comment

The treatment of radioactive wastes and their safe storage are problems of the next few decades and more distant future. One of the solutions considered for the long term involves the storage of the separated radionuclides in a crystalline matrix-like apatite (Carpéna & Lacout, 1993). Studies of this rather abundant natural mineral have shown good resistance of its structure to nuclear radiation damage (Carpéna & Mailhe, 1992; Carpéna, 1996). Replacing calcium with a radionuclide involves balancing the excess charge by substitution of anions or cations. Rare earth elements are good analogues to actinides and are used as model ions in nuclear chemistry. Britholite is one of the minerals with an apatite-type structure which includes rare earth ions. The electro-neutrality is maintained by substituting the phosphate with a silicate ion. The chemical stability makes the title compound, $(Ca_9,Nd)(PO_4)_5(SiO_4)F_2$, a good candidate for its intended use.

Comparison of the cell parameters of the title compound with those of fluorapatite ($a = 9.372$ and $c = 6.885$ Å; Sudarsanan *et al.*, 1972) and those of the rare earth silicate apatite $Nd_{9.33}(SiO_4)_6O_2$ ($a = 9.573$ and